THE JOURNAL OF BIOLOGICAL CHEMISTRY VOL. 289, NO. 19, pp. 13575–13588, May 9, 2014

Increased Glucose Metabolism and Glycerolipid Formation by Fatty Acids and GPR40 Receptor Signaling Underlies the Fatty Acid Potentiation of Insulin Secretion*

Received for publication, November 8, 2013, and in revised form, March 24, 2014 Published, JBC Papers in Press, March 27, 2014, DOI 10.1074/jbc.M113.531970

Mahmoud El-Azzouny[‡§], Charles R. Evans[‡], Mary K. Treutelaar[‡], Robert T. Kennedy[§¶], and Charles F. Burant[‡1]

From the Departments of [‡]Internal Medicine, [§]Chemistry, and [¶]Pharmacology, The University of Michigan, Ann Arbor, Michigan 48105

Background: Pathways underlying fatty acid potentiation of glucose-stimulated insulin secretion have not been fully elucidated.
Results: In INS-1 cells, fatty acids increase *de novo* production of glycerolipids and simultaneously increase glucose utilization. GPR40 receptor activation increases these activities.
Conclusion: Fatty acids enhance the production of multiple signals supporting glucose-stimulated insulin secretion.
Significance: The studies clarify the effects of fatty acids and GPR40 activity in β cell insulin secretion.

Acute fatty acid (FA) exposure potentiates glucose-stimulated insulin secretion in β cells through metabolic and receptor-mediated effects. We assessed the effect of fatty acids on the dynamics of the metabolome in INS-1 cells following exposure to [U-^{13}C]glucose to assess flux through metabolic pathways. Metabolite profiling showed a fatty acid-induced increase in long chain acyl-CoAs that were rapidly esterified with glucose-derived glycerol-3-phosphate to form lysophosphatidic acid, mono- and diacylglycerols, and other glycerolipids, some implicated in augmenting insulin secretion. Glucose utilization and glycolytic flux increased, along with a reduction in the NADH/NAD$^+$ ratio, presumably by an increase in conversion of dihydroxyacetone phosphate to glycerol-3-phosphate. The fatty acid-induced increase in glycolysis also resulted in increases in tricarboxylic cycle flux and oxygen consumption. Inhibition of fatty acid activation of FFAR1/GPR40 by an antagonist decreased glycerolipid formation, attenuated fatty acid increases in glucose oxidation, and increased mitochondrial FA flux, as evidenced by increased acylcarnitine levels. Conversely, FFAR1/GPR40 activation in the presence of low FA increased flux into glycerolipids and enhanced glucose oxidation. These results suggest that, by remodeling glucose and lipid metabolism, fatty acid significantly increases the formation of both lipid- and TCA cycle-derived intermediates that augment insulin secretion, increasing our understanding of mechanisms underlying β cell insulin secretion.

Glucose-stimulated insulin secretion (GSIS)[2] is mediated by a series of events that depend upon increases in glycolytic and tricarboxylic cycle (TCA) flux and the generation of metabolic coupling factors (1). Glycolytically derived ATP likely plays a role on the closure of K_{ATP} channels during the early phase of insulin secretion (1), and efficient glycolysis is dependent upon regeneration of NAD^+, at least in part via malate-aspartate and glycerol-3-phosphate shuttles (2). The TCA cycle is thought to participate in substrate cycling, which allows the generation of NADPH and other proposed intermediates that participate in the augmentation of insulin secretion (3).

Free fatty acids play an important role in regulating β cell function under physiological and pathological conditions. Exposure to fatty acid is known to amplify GSIS, with optimal potentiation dependent upon both fatty acid metabolism within the β cell (4, 5) and activation of the FFAR1/GPR40 receptor. Activation of this surface G protein-coupled receptor has been shown to be responsible for ~50% of the fatty acid potentiation effect of the second phase of GSIS in rat islets (6, 7). Both lipogenesis and lipolysis generate glycerolipids, such as DAG, which provides additional signals for potentiating GSIS (8). Fatty acids must be esterified to acyl-CoAs to function in GSIS potentiation. Inhibition of lipogenesis by triascin C, an acyl-CoA synthase inhibitor, inhibited FFA potentiation of insulin secretion in rat islets (9). Long chain acyl-CoA can act as a lipid signal for insulin exocytosis (10, 11), increase intracellular free calcium, and modulate K_{ATP} (12) and calcium channels (13). Increased formation of malonyl-CoA via mitochondrially derived citrate reduces fatty acid oxidation and enhances lipogenesis (5), increasing the availability of acyl-CoAs for metabolism. In addition, inhibition of lipase decreased phase 2 insulin secretion in rat islets (14), indicating a role for lipolysis in the

* This work was supported, in whole or in part, by National Institutes of Health Grants DK046960 (to R. T. K.), DK079084 (to C. F. B. and R. T. K.), and K25DK092558 (to C. R. E.). This work was also supported by Michigan Nutrition Obesity Research Center Grant P30 DK089503, by Michigan Diabetes Research and Training Center Grant P60 DK20572, by Michigan Regional Comprehensive Metabolomics Resource Core Grant U24 DK097153, by the Robert C. and Veronica Atkins Foundation (to C. F. B.), and by the A. Alfred Taubman Institute (to C. F. B).

[1] To whom correspondence should be addressed: Dept. of Internal Medicine, The University of Michigan, 6309 Brehm Tower, 1000 Wall St., Ann Arbor, MI, 48105-5714. Tel.: 734-615-3481; Fax: 734-232-8175; E-mail: burantc@umich.edu.

[2] The abbreviations used are: GSIS, glucose-stimulated insulin secretion; TCA, tricarboxylic acid; DAG, diacylglycerol; ACC, acetyl-CoA carboxylase; AMPK, AMP-activated protein kinase; PG, phosphatidylglycerol; Go3P, glycerol-3-phosphate; OCR, oxygen consumption rate(s); FFAR, FFA receptor; LPA, lysophosphatidic acid; 2PG, 2-phosphoglycerate; 3PG, 3-phosphoglycerate; ZMP, 5-aminoimidazole-4-carboxamide ribotide; G3P, glycerol-3-phosphate.

potentiation of insulin secretion. The decrease was reversed by palmitic acid, suggesting that lipolysis can be substituted by *de novo* generation of signaling lipids.

To our knowledge, there are no large scale assessments of metabolite changes in response to acute fatty acid exposure in β cells. In previous papers (15, 16), we have shown that INS-1 cells provide a tractable model for studying GSIS and assessments of flux through multiple metabolic pathways. Using these techniques, we assessed the changes in the INS-1 cell metabolome associated with fatty acid potentiation of GSIS. In addition to temporal changes in metabolites, we used both [U-^{13}C]glucose and [U-^{13}C]palmitate to follow remodeling of INS-1 cell metabolism in response to fatty acids and to synthetic FFAR1/GPR40 agonists and antagonists. The studies suggest that fatty acids enhance the flux of dihydroxyacetone phosphate to glycerol-3-phosphate, regenerating NAD^+, resulting in enhanced glycolytic and TCA cycle flux. We also provide evidence that FFAR1/GPR40 signaling enhances this flux, providing additional mechanisms for the positive pharmacological action of the FFAR1/GPR40 agonist (17, 18).

EXPERIMENTAL PROCEDURES

Materials—INS-1 832/3 cells (hereafter called INS-1 cells) were provided by Dr. Christopher Newgard (Duke University). All chemicals were purchased from Sigma-Aldrich unless noted otherwise.

Cell Culture and Media—INS-1 cells were cultured in RPMI medium as described previously (16). Cells were incubated in RPMI medium supplemented with 3 mM glucose for ~6 h prior to experimentation. Free fatty acid solution was prepared by finely grinding fatty acid (sodium palmitate) using a mortar and pestle and adding it to a warm solution of BSA (fatty acid-free) dissolved in Krebs-Ringer-HEPES buffer (20 mM HEPES, 118 mM NaCl, 5.4 mM KCl, 2.4 mM $CaCl_2$, 1.2 mM $MgSO_4$, and 1.2 mM KH_2PO_4 adjusted to pH 7.4 using sodium hydroxide) (16). Leaving the palmitate solution to stir using a magnetic stirrer for several hours at high speed yielded a homogenous suspension.

Glucose Stimulation—Palmitic or oleic acid (0.5 mM) was complexed with a 0.5% BSA (fatty acid-free) solution in KRHB buffer to achieve a 1:6 molar ratio of BSA to fatty acid. Cells were incubated for 30 min in glucose-free medium with BSA or palmitate or oleate before stimulation with 16.6 mM [^{12}C]glucose or [U-^{13}C]glucose for time periods ranging from 5–60 min. BSA or fatty acids were present throughout the incubation with glucose. At each time point, cells were snap-frozen using liquid nitrogen and kept at −80 °C until metabolite extraction, as described previously (15). At each time point, the medium was also collected for insulin measurement.

Fatty Acid Metabolism—Cells were incubated with 500 μM [U-^{13}C]palmitic acid (Sigma), 500 μM [U-^{13}C]oleic acid (Sigma), or 0.5% BSA (fatty acid-free) for 30 min in KRHB buffer with 0 mM glucose before stimulation with 16.7 mM [^{12}C]glucose for 60 min.

GPR40 Activation and Inhibition—Cells were incubated for 30 min with or without palmitate in the presence of either the FFAR1/GPR40 antagonist GW1100 (5 μM) or the FFAR1/GPR40 agonist Cay 10587 (10 μM) (Cayman Chemical, Ann Arbor, MI) or TAK 875 (5 μM) (Selleck Chemicals, Houston, TX). Drugs were dissolved in dimethyl sulfoxide, which was added alone for control studies.

Oxygen Consumption and Extracellular Acidification Rate Measurement—Measurements were performed using a SeaHorse XF24 extracellular flux analyzer (SeaHorse Bioscience) using 5× Krebs-Henseleit buffer as described by the manufacturer (555 mM NaCl, 23.5 mM KCl, 10 mM $MgSO_4$, and 6 mM Na_2HPO_4). Briefly, cells were seeded in 24 a Seahorse plate in full RPMI medium. RPMI medium was replaced with low-glucose RPMI medium 6 h before the experiment. The cells were incubated at 37 °C in the absence of CO_2 for 1 h, after which the medium was changed to KHB containing fatty acid or BSA before the assay. After equilibration, measurements were taken for 10 min, followed by the addition of 16.7 mM glucose for an additional 40 min for assessment of oxygen consumption.

Glucose Utilization—Cells were cultured in either 24- or 6-well plates and starved for 6 h in RPMI medium with 3 mM glucose before changing the medium to KRHB with no glucose for 30 min. This was followed by the addition of 16.7 mM glucose containing D-[5-^{3}H]glucose tracer. Cells were quenched and extracted as described in Ref. 19.

Insulin Measurement and Western Blot Analysis—For the insulin assay, a 100-μl aliquot of supernatant was assayed using a rat/mouse insulin ELISA kit (Millipore, Billerica, MA) after dilution with 1% BSA. Western blot analysis for phospho-ACC, phospho-AMPK, or β-actin (all from Cell Signaling Technology, Danvers, MA) was performed as described previously (16). The blot was quantified using ImageJ software (20).

Metabolite Measurement—Metabolites were extracted using 90% (9:1 methanol: chloroform)/10% water. Polar metabolites were separated using Luna NH_2, and lipids were separated using an Xbridge BEH C18 XP or Capcell C18 column (2 × 150 mm). Metabolites were detected by time of flight mass spectrometry in negative and positive mode as described previously (16). Untargeted analysis was performed using XCMS online (21), and metabolites were identified using accurate mass or authentic standards (if available) (16). Relative peak areas were used for the relative quantification of identified metabolites (16).

Statistics—Data are expressed as mean ± S.E. Statistical significance was determined, when appropriate, using unpaired, two-tailed Student's *t* test, assuming equal variance or analysis of variance using Tukey's post hoc analysis using SPSS. $p < 0.05$ was considered significant.

RESULTS

Metabolic Changes Associated with Fatty Acid-induced Potentiation of GSIS—INS-1 cells were preincubated with BSA or 500 μM palmitate complexed to BSA ("palmitate") for 30 min in 0 mM glucose, followed by stimulation with 16.6 mM glucose. Medium was collected for measurement of insulin secretion 0–60 min after the addition of glucose. Cell extracts were collected for determination of 69 metabolites by LC/MS prior to the addition of BSA or palmitate (−30 min (30 minutes before the stimulation with glucose)) or from the same cultures used to assess insulin secretion (0–60 min) (Fig. 1). As demonstrated

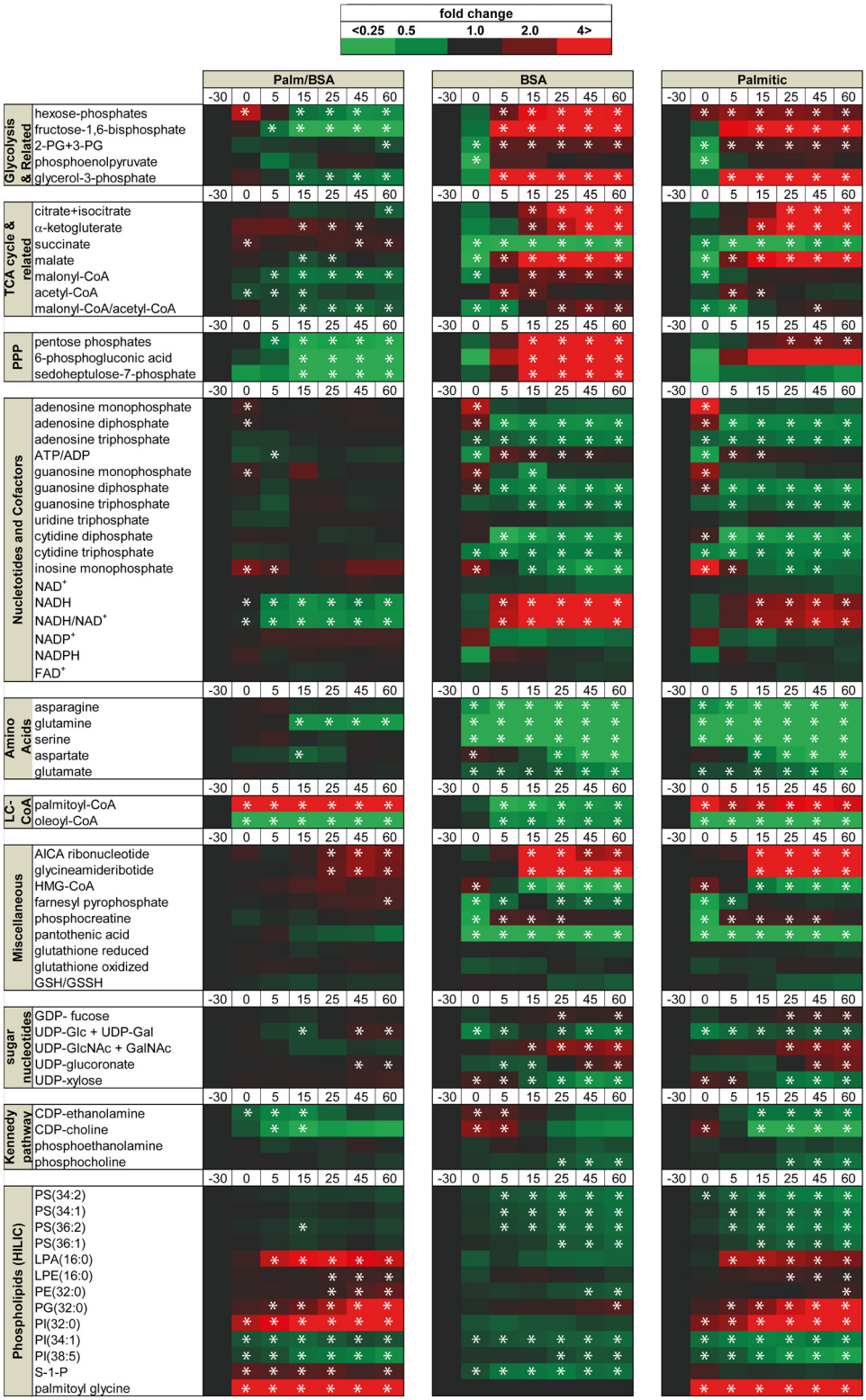

FIGURE 1. **Temporal metabolites profile of INS-1/832/3 cells upon glucose stimulation in the presence or absence of palmitic acid.** The heat maps (*center* and *right columns*) are showing the metabolites levels expressed as fold change of the (−30 min) time point. INS-1 cells were incubated in RPMI with 3 mM glucose for 6 h (−30 time point) before incubation in KRHB for 30 min with no glucose in the presence or absence of 500 μM palmitate (0 time point). Cells were stimulated with 16.6 mM [^{12}C]glucose for different time points (5–60 min). *, $p < 0.05$ in the peak areas, or their ratios, *versus* t = −30 min by analysis of variance using Tukey's post hoc analysis. The heat map in the *left column* shows the ratio of palmitate/BSA. *, $p < 0.05$ in the peak areas, or their ratios, between palmitate (*Palm*) or BSA at each time point by analysis of variance using Tukey's post hoc analysis. *PPP*, pentose phosphate pathway; *LC-CoA*, long chain-CoA; *HILIC*, lipids or phospholipids separated using hydrophilic interaction chromatography (HILIC).

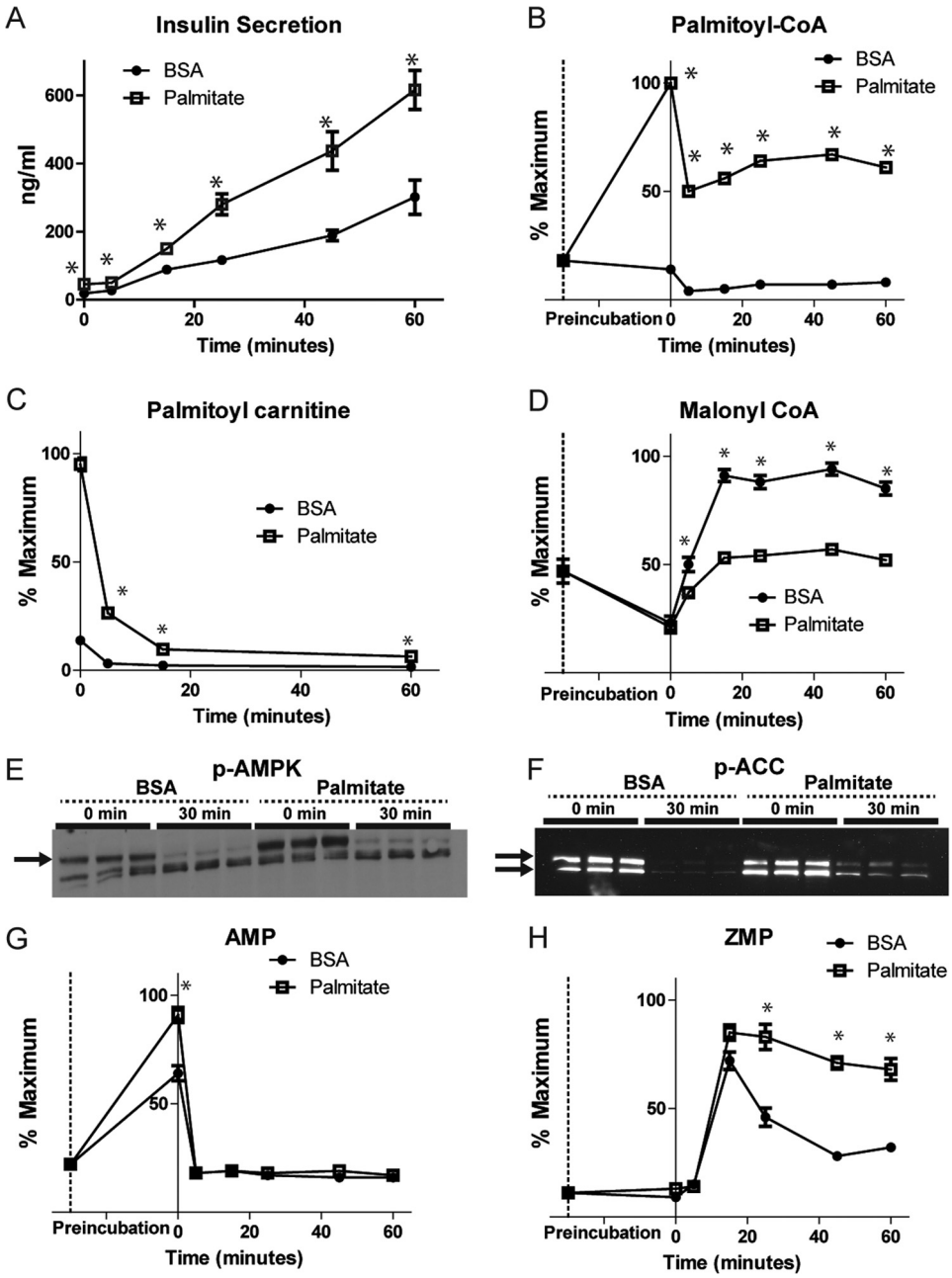

FIGURE 2. **Palmitic acid incubation effect on GSIS, AMPK, and related metabolites.** *A*, insulin levels after stimulation with 16.6 mM glucose for different time intervals in the presence or absence of 500 μM palmitate. Also shown are levels of palmitoyl-CoA (*B*), palmitoyl-carnitine (*C*), malonyl-CoA (*D*), AMP (*G*), and ZMP (*H*) before and after 30-min incubation with 500 μM palmitate (time 0) and after stimulation with 16.6 mM glucose for different time points. A Western blot analysis for *p*-AMPK (*E*) and *p*-ACC (*F*) before glucose addition (time 0) and after 30 min of glucose stimulation (30 min) is shown. *, $p < 0.05$ between BSA and palmitate at each time point. Points represent mean ± S.E. $n = 3–4$/time point.

previously in islets (4), preincubation of INS-1 cells with fatty acids potentiated GSIS ~2-fold at each time point compared with BSA controls (Fig. 2*A*). Heat maps of metabolite profiles (Fig. 1) showed that 30 min of preincubation with either BSA or palmitate in glucose-free medium resulted in lowering of the concentrations of most metabolites relative to preincubation levels, with the exception of expected rises in nucleotide monophosphate levels. As we (16) and others (22) have observed previously, palmitoyl-CoA decreased rapidly (~50%) following the addition of glucose in both BSA- and palmitate-pretreated cells (Fig. 2*B*). This observation is despite the marked increase in palmitoyl-CoA concentration following preincubation with palmitate (Fig. 2*B*). In addition, the concentration of palmitoylcarnitine declined rapidly (Fig. 2*C*), likely representing a reduction in the entry of palmitate into the mitochondria. The reduction in fatty acid entry into the mitochondria in β cells has been ascribed to elevations in malonyl-CoA, which inhibits CPT1 activity on the outer mitochondrial membrane (for a review, see Ref. 23). Indeed, in the absence of fatty acids, malonyl-CoA levels increase following glucose addition to INS-1 cells. However, in the presence of palmitate, the malonyl-CoA rise was blunted (Figs. 1 and 2*D*).

AMP-activated protein kinase (AMPK) is a known regulator of the glycerolipids/free fatty acid cycle (24, 25) and inhibits the

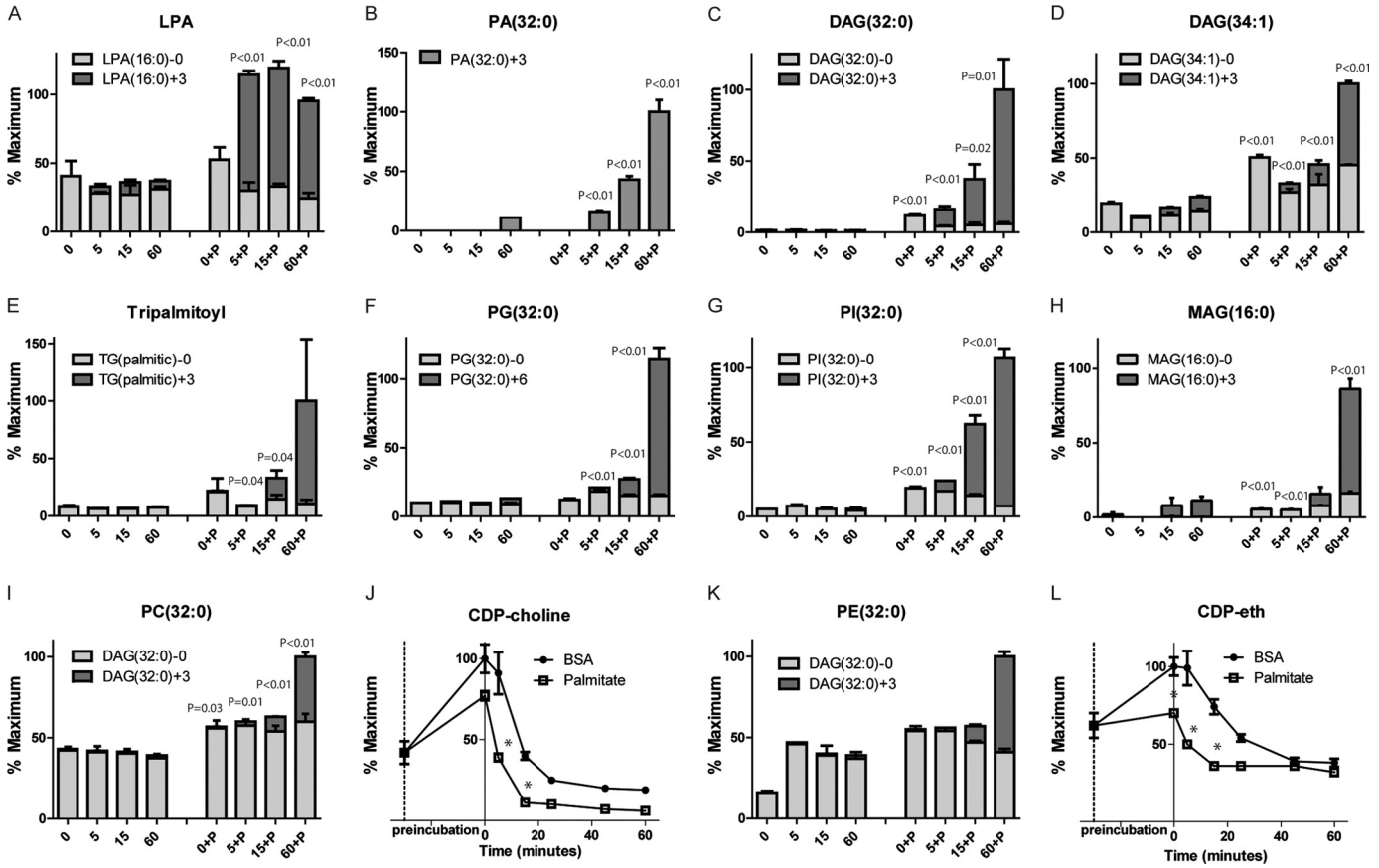

FIGURE 3. **Palmitic acid effect on carnitines and glycerolipids metabolites.** Glycerolipids levels before and after stimulation with 16.6 mM [U-^{13}C]glucose with and without preincubation with 500 μM palmitate for 30 min (time 0) and after 5, 15, or 60 min of glucose stimulation (*A–I* and *K*). CDP-choline (*J*) and CDP-ethanolamine (*CDP-eth*) (*L*) are measured after stimulation with [^{12}C]glucose. *, $p < 0.05$ between BSA and palmitate at each time point. *Error bars* represent mean ± S.E. $n = 3–4$.

formation of malonyl-CoA by phosphorylating ACC. We found that fatty acid addition increased the phosphorylation of AMPK and ACC (Fig. 2, *E* and *F*), increased AMP levels ~30% (Fig. 2*G*), and resulted in a small but persistent increase in *p*-ACC following glucose addition (Fig. 2*F*). Interestingly, ZMP, an AMP analog known to activate AMPK, also increased after glucose addition with both BSA and fatty acid. However, ZMP remained elevated through the time course of insulin secretion in cells exposed to palmitate (Fig. 2*H*), which may also contribute to the increased AMPK and ACC phosphorylation.

Fatty Acid Caused an Increase in de Novo-synthesized Glycerolipids—To assess the effect of fatty acids on the formation of glycerolipids, we used LC/MS to quantify a series of lipid-associated metabolites in INS-1 during GSIS using [U-^{13}C]glucose to track the *de novo* generation of glycerolipids containing palmitate. In the absence of added palmitate, a small rise was seen in the M+3 isotopologues of LPA, palmitic acid, DAG, triglycerides, phosphatidylglycerol (PG) and phosphatidylinositol, and monoacylglycerol (MAG) (Figs. 1 and 3, *A–H*). In contrast, total levels and M+3 isotopologues rose significantly in cells preincubated with palmitate (Fig. 3, *A–H*) with the rise in LPA preceding that of the other lipids, demonstrating a significant increase in the esterification of [U-^{13}C]glycerol-3-phosphate (Go3P) (Fig. 3, *A–H*). In INS-1 cells, the increase in DAG, suggested previously to play an important role in GSIS (6, 9), was primarily due to increases in M+3 species, suggesting that the bulk of DAG is generated *de novo* during GSIS in INS-1 cells. We also observed increases in the labeling of phosphatidylcholine and phosphatidylethanolamine and a parallel, rapid decrease in their precursor moieties, CDP-choline and CDP-ethanolamine, respectively (Fig. 3, *I–L*). A mass shift of M+3 is detected for all these metabolites, except for PG, which shows M+6 mass shifts, presumably because of the incorporation of two [^{13}C]Go3P molecules into the lipid.

Fatty Acid Exposure Increases Sphingosine-1-Phosphate and N-acyl Amide Levels—To further identify metabolites that could be implicated in fatty acid potentiation of GSIS, we used untargeted metabolomic profiling. We found significant increases in sphingosine-1-phosphate and two acylamides, palmitoyl taurine and palmitoyl glycine (Fig. 4, *A–C*), whose identities were confirmed by accurate mass and retention time matching with standards. Addition of taurine or glycine increased the levels of palmitoyl taurine and palmitoyl glycine, respectively, in the presence of palmitic acid (Fig. 4, *D* and *E*). Although significant increases in the palmitoylated species were observed, a minimal effect on basal or GSIS was found (Fig. 4*F*). Despite recent studies that suggest that acyltaurine species added exogenously to β cells enhanced GSIS (26), we did not detect changes in insulin secretion following the addition of taurine (data not shown) and, similarly, minimal effects of glycine.

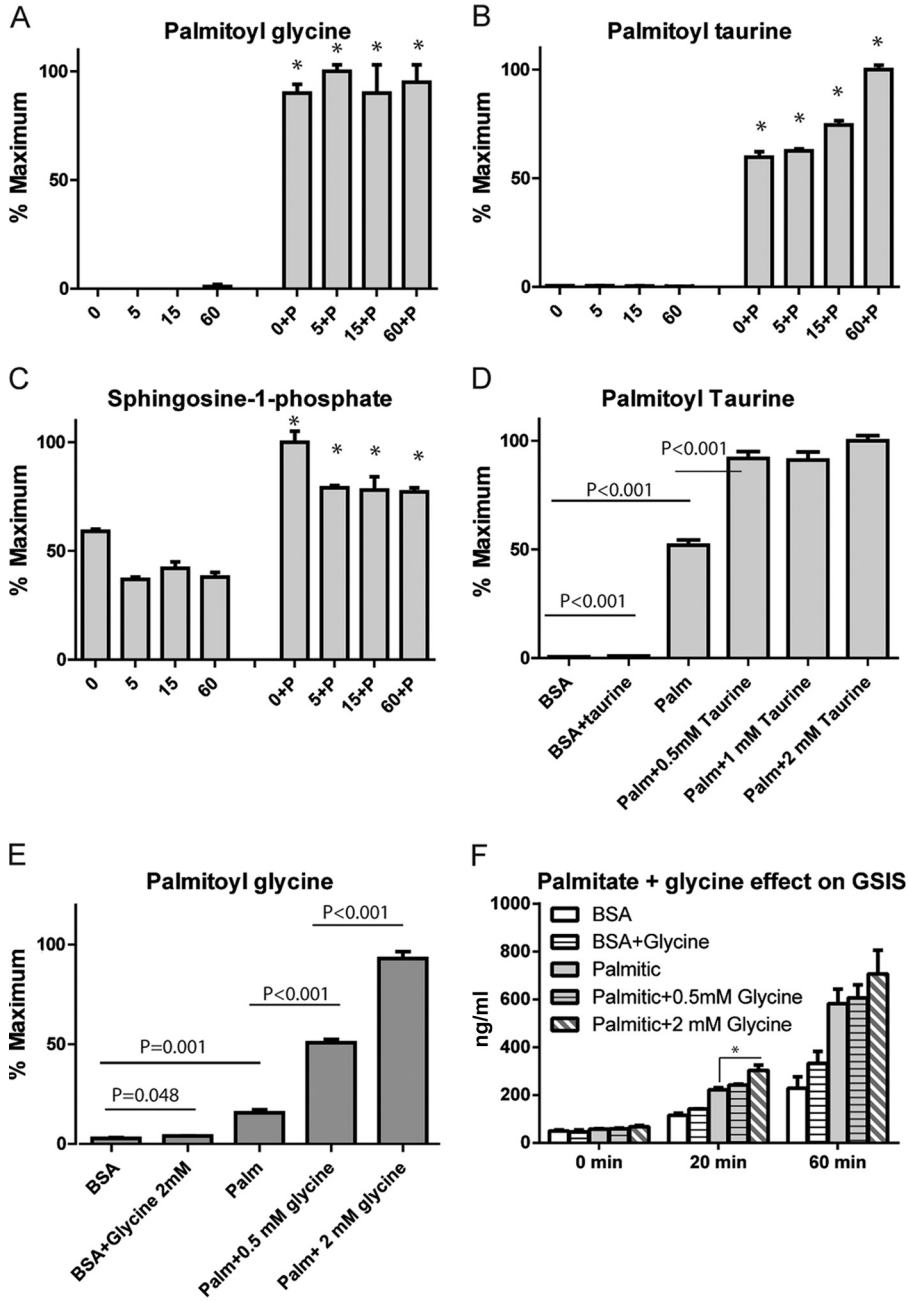

FIGURE 4. **Alterations in additional fatty acid identified by untargeted metabolomic profiling and effects on insulin secretion.** *A–C*, levels of palmitoyl glycine, palmitoyl taurine, and sphingosine phosphate after incubation with fatty acid for 30 min, followed by stimulation with 16.6 mM [U-^{13}C]glucose for 5,15, or 60 min. *D* and *E*, levels of palmitoyl taurine and palmitoyl glycine after the addition of increasing concentrations of their precursor amino acids in the presence or absence of palmitate. *F*, insulin levels after incubation of cells with BSA or palmitic acid in the presence or absence of glycine. Medium was collected before addition of glucose (0 min) or after stimulation with 16.6 mM glucose for 20 or 60 min. *Error bars* represent mean ± S.E. $n = 3–4$. *, $p < 0.05$ between BSA and palmitate at each time point unless described otherwise on the graph.

Fatty Acids Increase Glycolytic and TCA Cycle Carbon Flux—Following the addition of glucose, glycolytic and pentose phosphate intermediates rose as expected in both BSA- and palmitate-treated cells (Fig. 1). However, palmitate blunted this rise. By using [U-^{13}C]glucose, we found that the levels of fructose-bisphosphate fell (Fig. 5*A*) because of a reduction in ^{13}C-labeled intermediates (Fig. 5*B*). Similar findings were observed for other glycolytic intermediates (data not shown) as well as in the pentose phosphate intermediates such as 6-phsophoglucanate and ribose and ribulose-5P (not chromatographically resolved) (Fig. 5, *C–F*). Similar changes were seen in Go3P levels (Fig. 5, *G* and *H*). Palmitate did not affect the glucose-induced rise in 2PG + 3PG 2-phosphoglycerate + 3-phosphoglycerate (2PG + 3PG), which are not chromatographically resolved, or TCA cycle intermediates (Figs. 1 and 5, *I–K*).

Because we found an increase in the flux of glucose into glycerolipids in the presence of palmitate, we hypothesized that the reduction in the glycolytic intermediates was due to their rapid consumption. The conversion of dihydroxyacetone phosphate to Go3P utilizes NADH, and we observed a significant reduction of the NADH levels in palmitate-treated cells following the addition of glucose (Fig. 5*L*) as well as reduction in NADH/NAD$^+$ (Fig. 1).

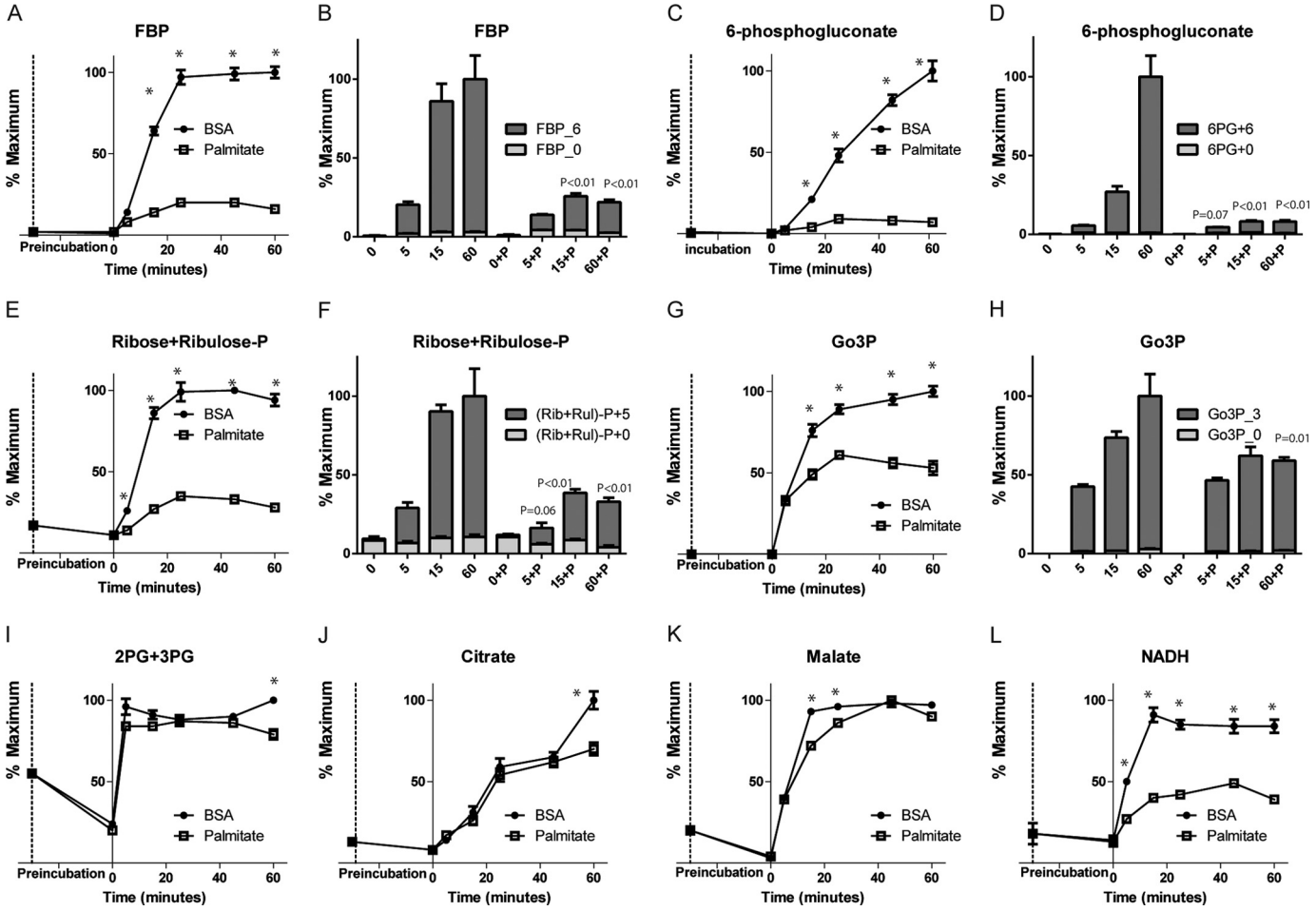

FIGURE 5. **Palmitic acid effect on glycolysis, pentose phosphate metabolites, and the TCA cycle.** Shown are changes in levels of fructose bisphosphate (*A*) phosphogluconate (*C*), ribose and ribulose-P (*E*), glycerol-3-phosphpate (*G*), 2PG + 3PG (*I*), citrate (*J*), malate (*K*), and NADH (*L*) after stimulation with 16.6 mM [^{12}C]glucose in the presence or absence of 500 μM palmitate. Also shown are changes in total mass and ^{13}C isotopologues after stimulation with 16.6 mM [U-^{13}C]glucose for fructose bisphosphate (*B*), phosphogluconate (*D*), ribose and ribulose-P (*F*), and glycerol-3-phosphate (*H*). *Error bars* represent mean ± S.E. $n = 3–4$, except for control at 60 min using [U-^{13}C]glucose, where $n = 2$. The values were confirmed with $n = 4$ in a separate experiment. *, $p < 0.05$ between BSA and palmitate at each time point.

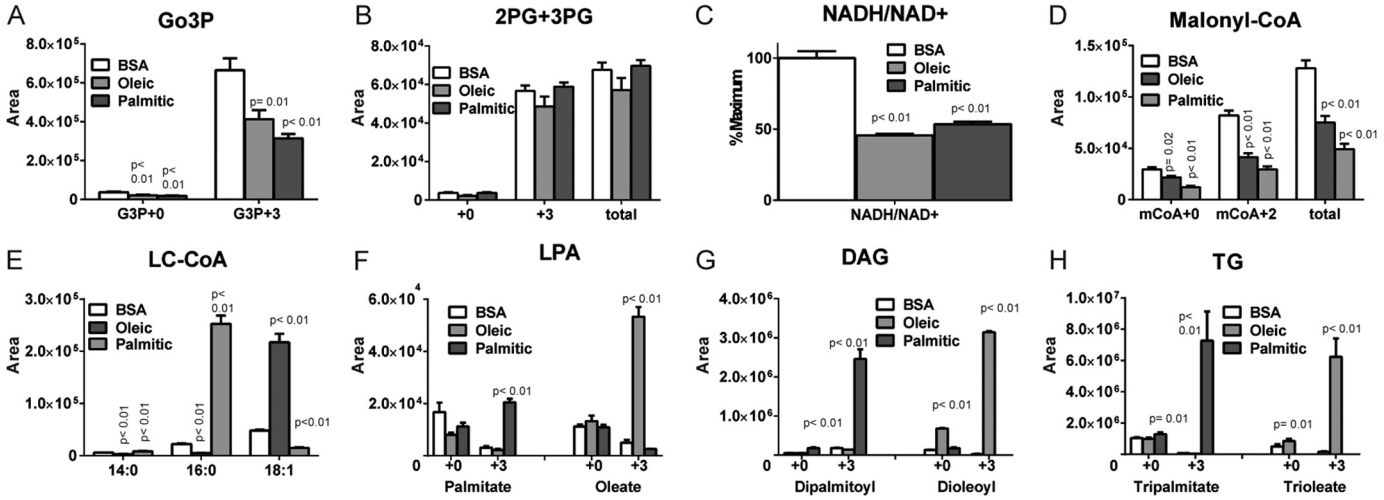

FIGURE 6. **Oleate and palmitate effect on different metabolites.** INS-1 832/13 cells were incubated in RPMI medium with low glucose for 6 h before incubation with either 500 μM palmitate, 500 μM oleate, or 0.5% BSA for 30 min. Preincubation was followed by stimulation with 16.6 mM [U-^{13}C]glucose for 60 min. Changes in the ^{13}C isotopologues are shown for glycerol-3-phosphate (*A*), 2PG + 3PG (*B*), NADH/NAD$^+$ (*C*), malonyl-CoA (*D*), long chain CoA (*E*), lysophosphatidic acid (*F*), diacylglycerol (*G*), and triglycerides (*H*). The relative peak area ± S.E. of the indicated metabolites was assessed. $n = 3–4$ for each metabolite.

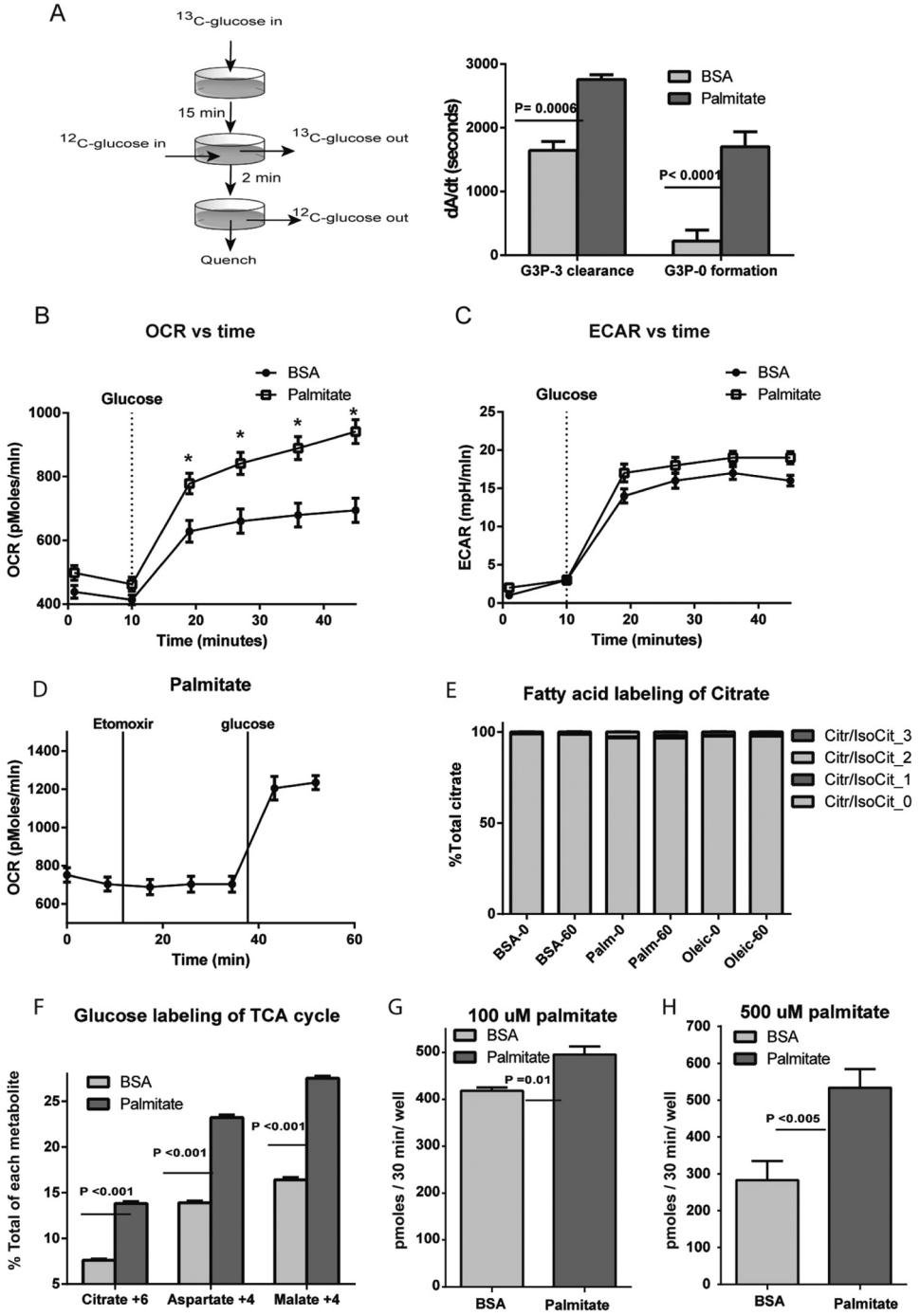

FIGURE 7. **Palmitic acid effect on glycolytic flux, fatty acid oxidation, oxygen consumption, and glucose utilization.** *A*, for the pulse-chase experiment, cells were stimulated with 16.7 mM [U-^{13}C]glucose for 15 min (pulse) before the KRHB was replaced with the same medium containing 16.7 mM [^{12}C]glucose for 2 min, after which the cells were quenched and the rate of consumption of labeled Go3P and the rate of formation of unlabeled Go3P in 2 min was plotted. *B* and *C*, the OCR and extracellular acidification rate were measured before and after the addition of 16.6 mM glucose. *D*, the OCR of cells incubated with 500 μM palmitate before the addition of 0.2 mM etomoxir followed by 16.7 mM glucose stimulation. *E*, the percentage labeling of citrate and isocitrate (*IsoCit*) after incubation of INS-1 cells with either BSA or [U-^{13}C]palmitate or [U-^{13}C]oleate for 30 min with no glucose (time 0) and after stimulation with 16.6 mM [^{12}C]glucose for 60 min (time 60). *Citr*, citrate. *F*, the percentage labeling of ultimate labeling of citrate, aspartate, and malate after 1-h treatment with [U-^{13}C]glucose. *G* and *H*, glucose utilization using 5-[^{3}H]glucose in the presence or absence of 100 or 500 μM palmitate. *Error bars* represent mean ± S.E. with $n = 3–4$ for metabolites analysis and $n = 10$ for SeaHorse experiments and $n = 3–10$ for glucose utilization. *, $p < 0.05$ between BSA and palmitate at each time point.

To confirm that these metabolic changes are not restricted to saturated fatty acids, we repeated the same experiment using INS-1 832/13 cells and pretreated cells with BSA, palmitate, or oleate. Oleate- and palmitate-treated cells showed similar reductions in M+3 [^{13}C]Go3P following the addition of [U-^{13}C]glucose (Fig. 6*A*) without changing 2PG + 3PG levels (Fig. 6*B*). NADH/NAD$^+$ (Fig. 6*C*) and malonyl-CoA (Fig. 6*D*) were also reduced. Oleate increased the levels of oleoyl-CoA (Fig. 6*E*) and oleoyl-LPA (Fig. 6*F*), dioleoyl DAG (Fig. 6*G*), and trioleol triglyceride (Fig. 6*H*), whereas palmitate formed the palmitoylated analogues of these lipid species (Fig. 6, *E–H*).

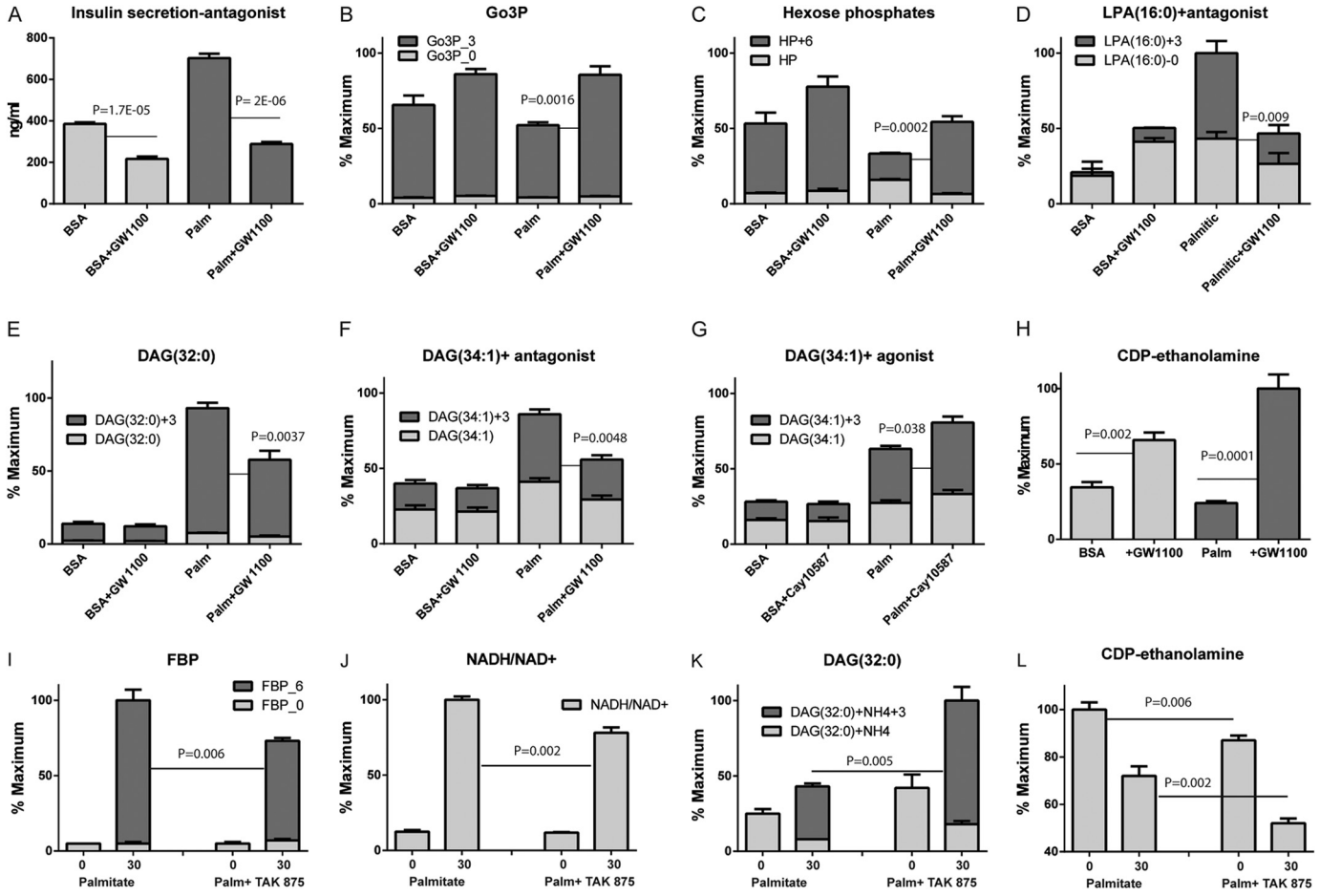

FIGURE 8. **GPR40 role in palmitic acid-induced metabolic changes.** INS-1 cells were incubated with 250 μM palmitate or 0.25% BSA in the presence or absence of 5 μM GPR40 antagonist (*GW1100*) for 30 min, followed by stimulation with 16.6 mM [U-^{13}C]glucose for 60 min. Using these conditions, the following were measured: insulin levels (*A*), changes in total mass and ^{13}C isotopologues of glycerol-3-phosphate (*B*), hexose phosphates (*C*), LPA (16:0) and DAG(32:0) (*E*), DAG (34:1) (*F*), and CDP-ethanolamine (*L*). INS-1 cells were incubated with 50 μM palmitate or BSA in the presence or absence of 10 μM Cay 10587 for 30 min, followed by stimulation with 16.6 mM [U-^{13}C]glucose for 60 min. *G*, accumulation of DAG (34:1). INS-1 cells were incubated with 50 μM palmitate or BSA in the presence or absence of 5 μM TAK 875 for 30 min, followed by stimulation with 16.6 mM [U-^{13}C]glucose for 30 min. Under these conditions, the following were measured: fructose bisphosphate (*FBP*) (*I*), NADH/NAD$^+$ ratio (*J*), DAG (32:0) (*K*), and CDP-ethanolamine (*L*). *Error bars* represent mean ± S.E. $n = 3–4$.

To confirm increased glucose flux to Go3P by fatty acid treatment, we performed a pulse-chase experiment in which a 15-min pulse of [U-^{13}C]glucose was chased for 2 min with unlabeled glucose in INS-1 cells pretreated with BSA or palmitate (Fig. 7*A*). The consumption of ^{13}C-labeled Go3P as well as the generation of unlabeled Go3P was faster in the presence of fatty acid (Fig. 7*A*), confirming a rapid increase of Go3P consumption following palmitate treatment.

As a consequence of the regeneration of NAD$^+$ following palmitate treatment, an increase glucose flux into the TCA cycle would be expected. Thus, we measured oxygen consumption in INS-1 cells pretreated with BSA or palmitate for 30 min. As shown in Fig. 7*B*, the addition of palmitate produced a small, statistically insignificant increase in oxygen consumption rates (OCR) prior to the addition of glucose. In contrast, following the addition of glucose, palmitate preincubation increased the OCR by ~66%, demonstrating an increase in glucose oxidation. Extracellular acidification rose following glucose addition but was not affected by palmitate pretreatment (Fig. 7*C*). The rise in extra cellular acidification rate, a measure of lactate production, was small, consistent with the low levels of lactate dehydrogenase in these cells (27). The OCR in INS-1 cells incubated with 500 μM palmitate was not changed by the addition of 0.2 mM etomoxir and did not prevent the rise in the OCR following glucose addition (Fig. 7*D*). The minimal contribution of palmitate to oxygen consumption in INS-1 cells was confirmed by the low levels of ^{13}C carbon incorporation into citrate following exposure of cells to [U-^{13}C]palmitate or [U-^{13}C]oleate in the presence or absence of glucose (Fig. 7*E*).

To further assess flux through the TCA cycle, cells were preincubated with BSA or palmitate and then, for 60 min, in the presence of [U-^{13}C]glucose. Measurement of the ratio of ^{13}C isotopologues of TCA intermediates revealed that fully labeled citrate (M+6), malate (M+4), and aspartate (M+4) were increased in the palmitate-pretreated cells by ~35% (Fig. 7*F*), supporting an increase of flux of glucose into the TCA cycle following palmitate treatment. Finally, to directly confirm that glucose utilization is increased with fatty acid treatment, we measured 5-[^{3}H]glucose utilization in the presence or absence of palmitate (Fig. 7*G–H*). Preincubation of palmitate at 100 and 500 μM palmitate increased glucose utilization by ~12 and 40%, respectively.

The GPR40 Receptor Modulates FFA Potentiation of GSIS and Fatty Acid Esterification—We next examined the role of the free fatty acid receptor FFAR1/GPR40 on metabolic flux in INS-1 cells.

We first preincubated cells with the FFAR1/GPR40 antagonist GW1100 in the presence or absence of 250 μM palmitate and measured insulin secretion and metabolite levels in response to the addition of 16.6 mM [U-^{13}C]glucose for 30 min. GSIS was decreased significantly by GW1100 inhibition of the GPR40 receptor, both in the absence and presence of palmitate (Fig. 8*A*), as described previously (7, 28). Metabolite analysis showed that palmitate reduced the concentration of M+6 hexose phosphates as well as M+3 Go3P, whereas GW1100-treated samples showed increased levels of M+6 hexoses (Fig. 8*B*) as well as M+3 Go3P isotopologues (Fig. 8*C*) following preincubation with palmitate. There was a parallel decrease in the accumulation of M+3 isotopologues of LPA (Fig. 8*D*) and various DAG species (Fig. 8, *E* and *F*) in antagonist-treated cells following palmitate addition. Conversely, the FFAR1/GPR40 agonist Cay 10587 increased the M+3 isotopologues of DAG, but only in the presence of 50 μM palmitate (Fig. 8*G*). CDP-ethanolamine increased in the presence of GPR40 antagonist (Fig. 8*H*), which is in agreement with our finding that an increase in CDP-ethanolamine may be a marker for decreased activity of the glycerolipids cycle.[3] We repeated these studies with TAK-875, which has shown clinical efficacy in phase II clinical trials (18). We found that, in the presence of [U-^{13}C]glucose and 50 μM palmitate, TAK-875 reduced the levels of fructose bisphosphate (Fig. 8*I*), and NADH/NAD$^+$ ratio (Fig. 8*J*), whereas it increased the M+3 isotopologues of DAG (Fig. 8*K*) and further reduced the levels of CDP-ethanolamine (Fig. 8*L*), indicative of increased activity of glycerolipid cycle and opposite that seen in the presence of the inhibitor.

Preincubation of INS-1 cells with GW1100 resulted in an ~2-fold increase in palmitoyl-carnitine levels, suggesting an increase in flux of palmitate into the mitochondria (Fig. 9*A*). The FFAR1/GPR40 agonist had no effect on palmitoyl-carnitine levels when cells were incubated with a low level (50 μM) of palmitate (Fig. 9*B*). These results suggest that flux into glycerolipids may be a primary determinant of fatty acid entry into mitochondria rather than modulation of CPT-1 by malonyl-CoA. Neither antagonist (Fig. 9*C*) nor agonist (Fig. 9*D*) affected palmitoyl-CoA accumulation in the absence of glucose, suggesting no effect of FFAR1/GPR40 receptors on fatty acid uptake or activation of the lipids by CoA synthase. To assess the effect of FFAR1/GPR40 activation on lipolysis, we incubated INS-1cells with [U-^{13}C]palmitate with or without agonist for 20 min in the absence of glucose. In the presence of agonist, there was an increase in the unlabeled DAG (34:1) and a decrease in the M+16/M+0 labeling ratio (Fig. 9*E*), consistent with previous reports of phospholipase C activation by the receptor (29). Similarly, using [U-^{13}C]palmitate and unlabeled glucose, TAK-875 increased the levels of both labeled and unlabeled DAG, also consistent with an increase in both lipogenesis and lipolysis (Fig. 9*F*).

Finally, we assessed the effect of FFAR1/GPR40 receptor manipulation on palmitate-stimulated glucose oxidation in INS-1 cells. In the presence of agonist, there was a further increase in glucose oxidation in the presence of palmitate and Cay 10587 (Fig. 9*G*). Conversely, the augmentation of glucose oxidation by palmitate was reduced by the FFAR1/GPR40 receptor antagonist (Fig. 9*H*). This suggests that FFAR1/GPR40 activation enhances the intrinsic metabolic remodeling of glucose metabolism by fatty acids.

DISCUSSION

The secretion of insulin is primarily regulated by the entry of glucose into the β cell but is modulated by the nervous system and hormonal and nutritive inputs (30). Fatty acids augment insulin release *in vivo* and *in vitro*, and its effects have been shown to be mediated via intracellular metabolism and through surface receptors (8). In this report, we show that a 30-min incubation of INS-1 cells with palmitate prior to the addition of glucose results in a doubling of insulin release, as seen previously in intact islets (4). Prior to glucose addition, palmitate exposure results in an ~7-fold increase in intracellular palmitoyl-CoA and a small increase in oxygen consumption but little effect on basal insulin secretion and minimal changes in the majority of intracellular metabolites, with the exception of a significant increase in the formation of palmitoyl-carnitine, likely generated by the flux of fatty acid into the mitochondria. This suggests that, despite a small increase in TCA cycle activity, there is a minimal generation of factors necessary for insulin secretion. Following the addition of [U-^{13}C]glucose, palmitoyl-CoA rapidly declines with the formation M+3 LPA and DAG isotopologues containing palmitate, directly demonstrating that acyl-CoAs are rapidly esterified to Go3P derived from extracellular glucose. This effect is not limited to saturated fatty acids because identical changes are seen following preincubation of INS-1 cells with oleic acid (Fig. 6).

The esterification of fatty acids with Go3P has several effects that appear to contribute to their ability to augment insulin secretion. We identified an increased glycolytic flux toward Go3P (Fig. 7*A*), reduced NADH levels, and a decrease in the NADH/NAD$^+$ ratio following fatty acid addition (Figs. 1 and 4). As suggested previously (31), we show directly that fatty acid addition increases glycolytic (Fig. 7*A*) and TCA cycle (Fig. 7*F*) flux, glucose utilization (Fig. 7, *G* and *H*), and glucose oxidation (Fig. 7*B*). Each should result in the generation of additional stimulus-secreting coupling factors that have been suggested to arise from the mitochondrial metabolism in β cells (1). Although fatty acids increased glucose oxidation, glucose addition reduced fatty acid entry and oxidation in mitochondria, as indicated by the fall in C16 acylcarnitine levels (Fig. 2*C*). The reduction in fatty acid mitochondrial uptake has been attributed to increases in malonyl-CoA inhibition of CPT-1. Although malonyl-CoA levels rise with glucose, fatty acid addition results in a significant blunting of the rise in malonyl-CoA in INS-1 cells (Fig. 2*D*). The reason for the reduction is not clear, but decreased export of citrate/isocitrate from the mitochondria or an increase in consumption for *de novo* lipogenesis may play a role. These results also suggest that the decrease in fatty acid oxidation following glucose addition may be primarily due to the redirection of acyl-CoA toward esterification rather than blocking of the influx to the mitochondria via CPT1 inhibition by malonyl-CoA.

[3] M. El-Azzouny, C. R. Evans, M. K. Treutelaar, R. T. Kennedy, and C. F. Burant, unpublished data.

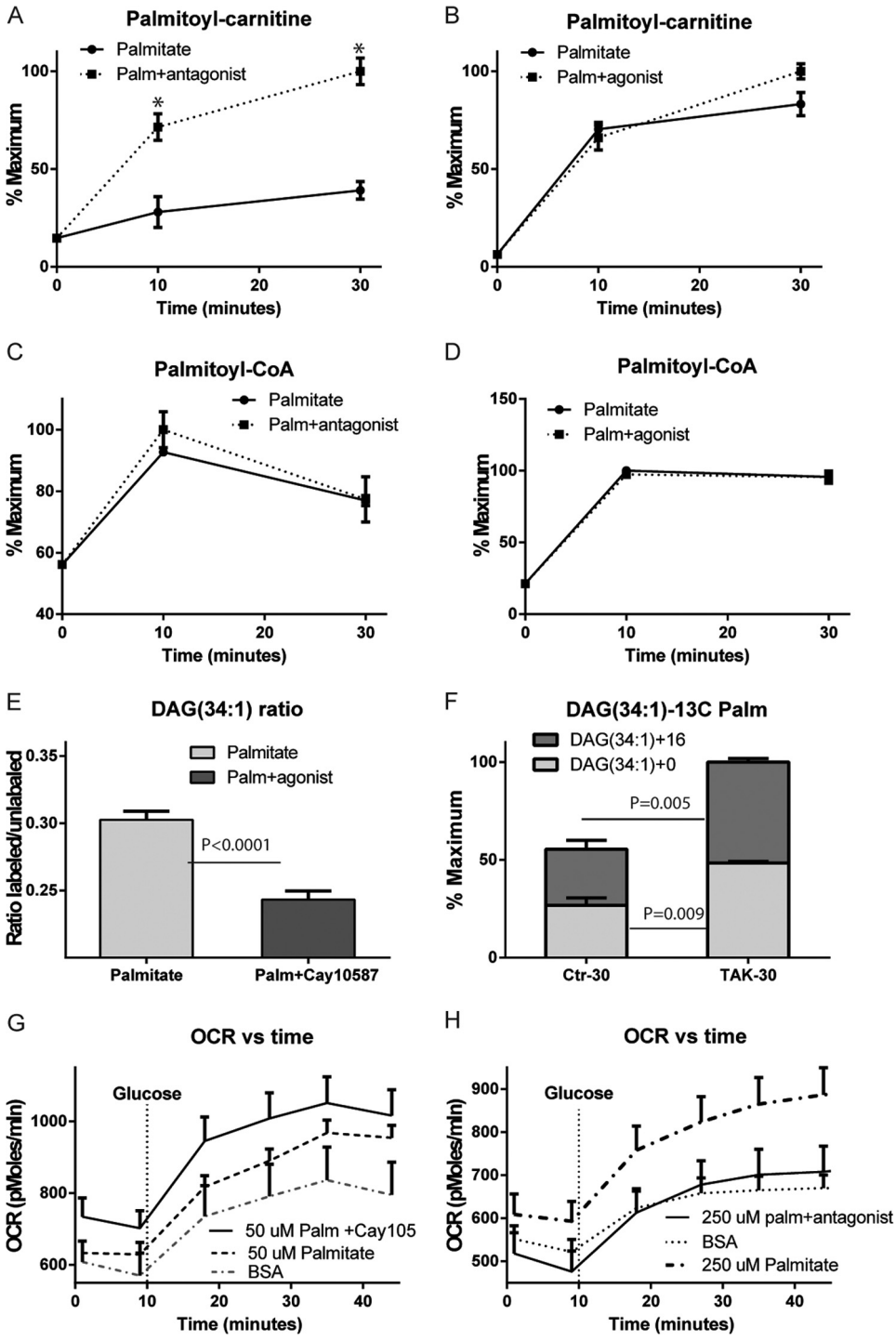

FIGURE 9. **Metabolic changes with GPR40 modulation.** INS-1 cells were incubated with 250 μM palmitate ± 5 μM GW1100 in the absence of glucose for 30 min, and the levels of palmitoyl-carnitine (*A*) and palmitoyl-CoA (*C*) were measured at different time points. INS-1 cells were incubated with 50 μM palmitate ± 10 μM Cay 10587 GPR40 agonist in the absence of glucose for 30 min, and the levels of palmitoyl-carnitine (*B*) and palmitoyl-CoA (*D*) were measured at different time points. *I–L*, INS-1 cells were incubated with 50 μM palmitate in the presence or absence of 5 μM TAK 875. *E*, INS-1 cells were incubated with 50 μM [U-^{13}C]palmitate (*Palm*) in the absence of glucose ± Cay 10587 agonist for 30 min, and the ratio of labeled DAG (34:1)+16 to unlabeled DAG (34:1) was measured. *F*, INS-1 cells were incubated with 50 μM [U-^{13}C]palmitate in the absence of glucose ± TAK 875 for 30 min before stimulation with [^{12}C]glucose for another 30 min, and the change in total mass and ^{13}C isotopologues of labeled DAG (34:1) was measured. Shown is the oxygen consumption rate in the presence or absence of agonist (*Cay10587*) (*G*) or antagonist (*GW1100*) (*H*) before and after stimulation with 16.6 mM glucose. *Error bars* represent mean ± S.E. $n = 3$ or 4 for metabolite analysis and $n = 6–7$ for the SeaHorse experiment. *, $p < 0.05$.

The increase in *de novo* lipogenesis resulted in the generation of a variety of lipid intermediates that have been described as candidate signals for insulin secretion (8). Lipogenesis is part of the larger glycerolipid-free fatty acid cycle, which is activated by glucose in β cells, and there is evidence that both the lipogenic and lipolytic arms of the cycle supply important signaling molecules (23). In glucose-responsive INS-1 cells, we find that the majority of increases in whole cell lipid intermediates, includ-

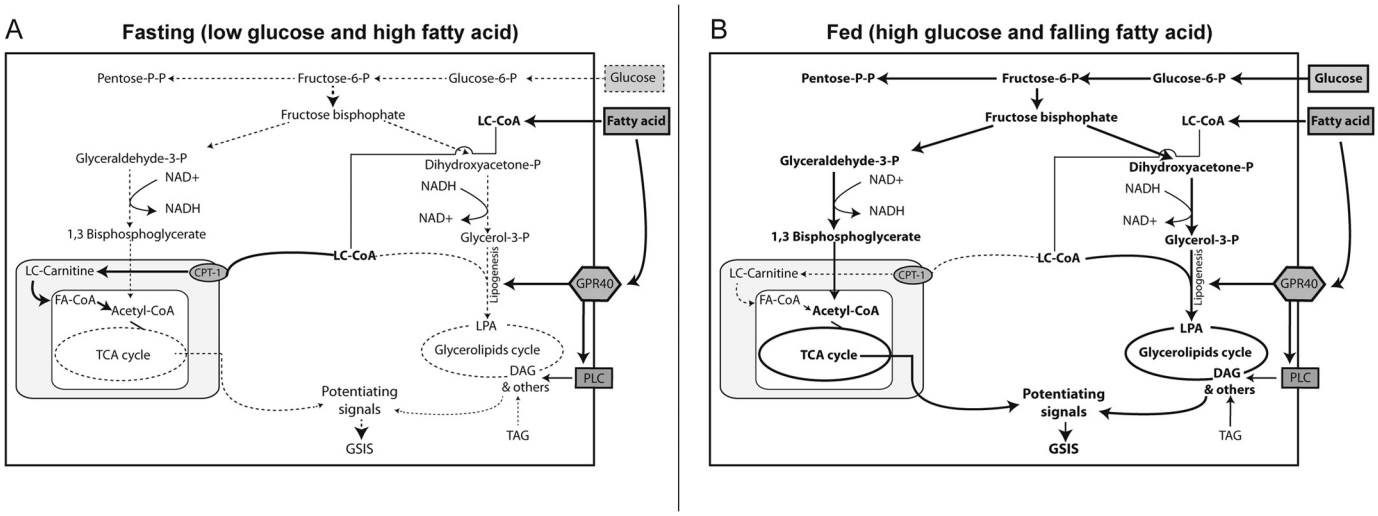

FIGURE 10. **Proposed pathways for fatty acid metabolism during the fed and fasting state and its role in potentiating insulin secretion.** In β cells, fatty acids increase glucose flux to glycerol-3-phosphate (*Glycerol-3-P*) to increase formation of lysophosphatidic acid (LPA) and downstream signaling molecules. The increased conversion of dihydroxyacetone phosphate regenerates NAD^+, which increases glycolytic flux and increases TCA cycle activity. FFAR1/GPR40 receptor activation appears to enhance the formation of LPA and increase glycerolipid cycling. *LC-CoA*, long chain CoA.

ing LPA, palmitic acid, DAG, PG, phosphatidylinositol, and monoacylglycerol, arise from the lipogenesis pathway because little increases in M+0 isotopologues are found, even after 60 min of glucose stimulation. DAG has multiple potential roles in insulin secretion, including activation of Munc13-1, a receptor known to amplify insulin exocytosis (32, 33) and activation of protein kinase D1 (PKD1), which modulates the reorganization of the cortical actin network, perhaps playing a role in the second phase of insulin secretion (6). Recently, Prentki *et al.* (23) have suggested that increases in monoacylglycerol as well as DAG in β cells can activate Munc13-1.

In addition to lipid species identified previously, we found marked increases in cellular content of various acylamides. These fatty acid derivatives have not been reported previously in β cells, and their effect is unknown. Acylamides have been found in neuronal tissue and reportedly possess various functions (34, 35), including modulation of calcium flux, nitric oxide generation (36), and transient receptor potential (TRP) calcium channels (37). Although we were able to increase the intracellular concentration of those metabolites by increasing the levels of their amino acid precursors, this did not result in alterations in insulin secretion. Interestingly, taurine has been suggested to restore β cell insulin secretion following chronic fatty acid exposure. However, this beneficial effect was attributed to its antioxidant ability (38).

The activation of the FFAR1/GPR40 receptor mediates about 50% of the augmentation of insulin secretion by fatty acid (7). As indicated above, FFAR1/GPR40 has been proposed to increase β cell calcium and activate phospholipase C-generating diacylglycerols, which may tether PKD1 to the plasma membrane increasing its activity (6), although the latter has not been demonstrated directly in β cells. We sought to determine whether acute modulation of FFAR1/GPR40 had an effect on the β cell metabolome. Inhibiting FFAR1/GPR40 receptors resulted in attenuation of the free fatty acid augmentation of *de novo* DAG synthesis. It also decreased oxygen consumption by INS-1 cells and decreased insulin secretion. In contrast, FFAR1/GPR40 agonists increased the flux of glucose and palmitate into DAG, increased lipolysis, and increased oxygen consumption. The increase in palmitoyl carnitine levels following disruption of GPR40 signaling reflects increased fatty acid influx into mitochondria. The redirection of fatty acids into the mitochondria for oxidation by overexpression of CPT-1 has been shown to be associated with an attenuation of insulin secretion (39, 40), and this redirection is associated with decreased glycerolipid formation (39). Thus, it appears that GPR40 activation is important for augmenting the partitioning of fatty acids to the glycerolipid pathway and fatty acid enhancement of GSIS.

These data are also in agreement with studies that show that the GPR40 agonist TAK-875 is more effective in the presence of fatty acids to increase insulin secretion (41), although they attribute the augmentation to enhanced binding of the agonist to the receptor. However, our data are somewhat at odds with a previous study by Alquier *et al.* (42) examining glucose and fatty acid utilization in islets isolated from $GPR40^{-/-}$ mice. Consistent with our data, the authors saw no effect of GPR40 disruption on glucose utilization in the absence of fatty acids, although glucose utilization was not assessed in the presence of fatty acids. However, they saw no reduction in the incorporation of palmitate into total lipids. This may reflect our direct assessment of ^{13}C label flux into specific glycerolipids or might indicate intrinsic differences between islets and INS-1 cells or the potential for adaptation of islets following disruption of GPR40 in mice. The development of a specific methodology to estimate metabolite flux in intact rodent islets will help clarify these potential differences.

In summary, our data suggest that FFAR1/GPR40 enhances the intrinsic effects of fatty acids to remodel the intermediary metabolism to augment insulin secretion. This effect does not appear to be due to increased uptake or activation of fatty acid because disruption of FFAR1/GPR40 did not alter the levels of palmitoyl-CoA in INS-1 cells. At present, it is unclear how the activity of the pathways leading to *de novo* lipogenesis occurs following FFAR1/GPR40 activation, but modulation of G3P

acyltransferase (GPAT) activity may be a target, given the increased flux into the early steps of the lipogenic pathway. Our data are also consistent with the idea that, in the fasting state, plasma fatty acids increase, leading to increased long chain acyl-CoA levels in β cells. Although glucose and fatty acid oxidation is occurring, there is minimal generation of coupling factors to increase insulin secretion (Fig. 10*A*). As glucose levels rise after feeding, the presence of fatty acids increases esterification with glycerol-3-phosphate, resulting in an increased flux to glycolipids and the formation of lipid-derived factors important in insulin secretion (Fig. 10*B*). The increased flux increases regeneration of NAD^+, accelerating glycolysis and flux into the TCA cycle above that which would occur following exposure to glucose alone. Our data also suggests that, in addition to the activation of the PLC-PKD1 pathway described previously (6), FFAR1/GPR40 activation also enhances flux through the glycerolipid pathway, augmenting the formation of coupling factors. This may be important because fatty acid entry into the β cell likely falls as plasma fatty acids decrease following a meal because of insulin-mediated reduction in lipolysis in fat cells. Thus, activation of the FFAR1/GPR40 receptor by fatty acids or receptor agonists (18) may ensure continued fatty acid esterification and the provision of signaling lipids for insulin secretion.

Acknowledgments—We thank Katherine Overmyer for discussions, Dr. Heidi Iglay Reger for assistance with statistical analysis, Sydney Bridges for performing the SeaHorse analysis, and Dr. Ian Sweet for providing unpublished data for review.

REFERENCES

1. Jitrapakdee, S., Wutthisathapornchai, A., Wallace, J. C., and MacDonald, M. J. (2010) Regulation of insulin secretion: role of mitochondrial signalling. *Diabetologia* **53,** 1019–1032
2. Bender, K., Newsholme, P., Brennan, L., and Maechler, P. (2006) The importance of redox shuttles to pancreatic β-cell energy metabolism and function. *Biochem. Soc. Trans.* **34,** 811–814
3. Jensen, M. V., Joseph, J. W., Ronnebaum, S. M., Burgess, S. C., Sherry, A. D., and Newgard, C. B. (2008) Metabolic cycling in control of glucose-stimulated insulin secretion. *Am. J. Physiol. Endocrinol. Metab.* **295,** E1287–97
4. Parker, S. M., Moore, P. C., Johnson, L. M., and Poitout, V. (2003) Palmitate potentiation of glucose-induced insulin release: a study using 2-bromopalmitate. *Metabolism* **52,** 1367–1371
5. Nolan, C. J., Madiraju, M. S., Delghingaro-Augusto, V., Peyot, M. L., and Prentki, M. (2006) Fatty acid signaling in the β-cell and insulin secretion. *Diabetes* **55,** S16–23
6. Ferdaoussi, M., Bergeron, V., Zarrouki, B., Kolic, J., Cantley, J., Fielitz, J., Olson, E. N., Prentki, M., Biden, T., MacDonald, P. E., and Poitout, V. (2012) G protein-coupled receptor (GPR)40-dependent potentiation of insulin secretion in mouse islets is mediated by protein kinase D1. *Diabetologia* **55,** 2682–2692
7. Latour, M. G., Alquier, T., Oseid, E., Tremblay, C., Jetton, T. L., Luo, J., Lin, D. C., and Poitout, V. (2007) GPR40 is necessary but not sufficient for fatty acid stimulation of insulin secretion *in vivo*. *Diabetes* **56,** 1087–1094
8. Prentki, M., and Madiraju, S. R. (2012) Glycerolipid/free fatty acid cycle and islet β-cell function in health, obesity and diabetes. *Mol. Cell Endocrinol.* **353,** 88–100
9. Roduit, R., Nolan, C., Alarcon, C., Moore, P., Barbeau, A., Delghingaro-Augusto, V., Przybykowski, E., Morin, J., Massé, F., Massie, B., Ruderman, N., Rhodes, C., Poitout, V., and Prentki, M. (2004) A role for the malonyl-CoA/long-chain acyl-CoA pathway of lipid signaling in the regulation of insulin secretion in response to both fuel and nonfuel stimuli. *Diabetes* **53,** 1007–1019
10. Deeney, J. T., Gromada, J., Høy, M., Olsen, H. L., Rhodes, C. J., Prentki, M., Berggren, P. O., and Corkey, B. E. (2000) Acute stimulation with long chain acyl-CoA enhances exocytosis in insulin-secreting cells (HIT T-15 and NMRI β-cells). *J. Biol. Chem.* **275,** 9363–9368
11. Corkey, B. E., Deeney, J. T., Yaney, G. C., Tornheim, K., and Prentki, M. (2000) The role of long-chain fatty acyl-CoA esters in β-cell signal transduction. *J. Nutr.* **130,** 299S-304S
12. Bränström, R., Aspinwall, C. A., Välimäki, S., Ostensson, C. G., Tibell, A., Eckhard, M., Brandhorst, H., Corkey, B. E., Berggren, P. O., and Larsson, O. (2004) Long-chain CoA esters activate human pancreatic β-cell KATP channels: potential role in type 2 diabetes. *Diabetologia* **47,** 277–283
13. Tian, Y., Corkey, R. F., Yaney, G. C., Goforth, P. B., Satin, L. S., and Moitoso de Vargas, L. (2008) Differential modulation of L-type calcium channel subunits by oleate. *Am. J. Physiol. Endocrinol. Metab.* **294,** E1178–86
14. Mulder, H., Yang, S., Winzell, M. S., Holm, C., and Ahrén, B. (2004) Inhibition of lipase activity and lipolysis in rat islets reduces insulin secretion. *Diabetes* **53,** 122–128
15. Lorenz, M. A., Burant, C. F., and Kennedy, R. T. (2011) Reducing time and increasing sensitivity in sample preparation for adherent mammalian cell metabolomics. *Anal. Chem.* **83,** 3406–3414
16. Lorenz, M. A., El Azzouny, M. A., Kennedy, R. T., and Burant, C. F. (2013) Metabolome response to glucose in the β-cell line INS-1 832/13. *J. Biol. Chem.* **288,** 10923–10935
17. Burant, C. F. (2013) Activation of GPR40 as a therapeutic target for the treatment of type 2 diabetes. *Diabetes Care* **36,** S175–9
18. Burant, C. F., Viswanathan, P., Marcinak, J., Cao, C., Vakilynejad, M., Xie, B., and Leifke, E. (2012) TAK-875 *versus* placebo or glimepiride in type 2 diabetes mellitus: a phase 2, randomised, double-blind, placebo-controlled trial. *Lancet* **379,** 1403–1411
19. Malmgren, S., Nicholls, D. G., Taneera, J., Bacos, K., Koeck, T., Tamaddon, A., Wibom, R., Groop, L., Ling, C., Mulder, H., and Sharoyko, V. V. (2009) Tight coupling between glucose and mitochondrial metabolism in clonal β-cells is required for robust insulin secretion. *J. Biol. Chem.* **284,** 32395–32404
20. Schneider, C. A., Rasband, W. S., and Eliceiri, K. W. (2012) NIH Image to ImageJ: 25 years of image analysis. *Nat. Methods* **9,** 671–675
21. Tautenhahn, R., Patti, G. J., Rinehart, D., and Siuzdak, G. (2012) XCMS online: a web-based platform to process untargeted metabolomic data. *Anal. Chem.* **84,** 5035–5039
22. Prentki, M., Vischer, S., Glennon, M. C., Regazzi, R., Deeney, J. T., and Corkey, B. E. (1992) Malonyl-CoA and long chain acyl-CoA esters as metabolic coupling factors in nutrient-induced insulin secretion. *J. Biol. Chem.* **267,** 5802–5810
23. Prentki, M., Matschinsky, F. M., and Madiraju, S. R. (2013) Metabolic signaling in fuel-induced insulin secretion. *Cell Metabolism* **18,** 162–185
24. Hardie, D. G. (2011) Sensing of energy and nutrients by AMP-activated protein kinase. *Am. J. Clin. Nutr.* **93,** 891S-6
25. Hardie, D. G. (2008) AMPK: a key regulator of energy balance in the single cell and the whole organism. *Int. J. Obes.* **32,** S7–12
26. Waluk, D. P., Vielfort, K., Derakhshan, S., Aro, H., and Hunt, M. C. (2013) N-Acyl taurines trigger insulin secretion by increasing calcium flux in pancreatic β-cells. *Biochem. Biophys. Res. Commun.* **430,** 54–59
27. Sekine, N., Cirulli, V., Regazzi, R., Brown, L. J., Gine, E., Tamarit-Rodriguez, J., Girotti, M., Marie, S., MacDonald, M. J., and Wollheim, C. B. (1994) Low lactate dehydrogenase and high mitochondrial glycerol phosphate dehydrogenase in pancreatic β-cells. Potential role in nutrient sensing. *J. Biol. Chem.* **269,** 4895–4902
28. Briscoe, C. P., Peat, A. J., McKeown, S. C., Corbett, D. F., Goetz, A. S., Littleton, T. R., McCoy, D. C., Kenakin, T. P., Andrews, J. L., Ammala, C., Fornwald, J. A., Ignar, D. M., and Jenkinson, S. (2006) Pharmacological regulation of insulin secretion in MIN6 cells through the fatty acid receptor GPR40: identification of agonist and antagonist small molecules. *Br. J. Pharmacol.* **148,** 619–628
29. Mancini, A. D., and Poitout, V. (2013) The fatty acid receptor FFA1/GPR40 a decade later: how much do we know? *Trends Endocrinol. Metab.* **24,** 398–407
30. Rorsman, P., and Braun, M. (2013) Regulation of insulin secretion in hu-

man pancreatic islets. *Annu. Rev. Physiol.* **75,** 155–179
31. Prentki, M., and Madiraju, S. R. (2008) Glycerolipid metabolism and signaling in health and disease. *Endocr. Rev.* **29,** 647–676
32. Kwan, E. P., Xie, L., Sheu, L., Nolan, C. J., Prentki, M., Betz, A., Brose, N., and Gaisano, H. Y. (2006) Munc13–1 deficiency reduces insulin secretion and causes abnormal glucose tolerance. *Diabetes* **55,** 1421–1429
33. Sheu, L., Pasyk, E. A., Ji, J., Huang, X., Gao, X., Varoqueaux, F., Brose, N., and Gaisano, H. Y. (2003) Regulation of insulin exocytosis by Munc13–1. *J. Biol. Chem.* **278,** 27556–27563
34. Tan, B., O'Dell, D. K., Yu, Y. W., Monn, M. F., Hughes, H. V., Burstein, S., and Walker, J. M. (2010) Identification of endogenous acyl amino acids based on a targeted lipidomics approach. *J. Lipid Res.* **51,** 112–119
35. Tan, B., Yu, Y. W., Monn, M. F., Hughes, H. V., O'Dell, D. K., and Walker, J. M. (2009) Targeted lipidomics approach for endogenous *N*-acyl amino acids in rat brain tissue. *J. Chromatogr. B. Analyt. Technol. Biomed. Life. Sci.* **877,** 2890–2894
36. Rimmerman, N., Bradshaw, H. B., Hughes, H. V., Chen, J. S., Hu, S. S., McHugh, D., Vefring, E., Jahnsen, J. A., Thompson, E. L., Masuda, K., Cravatt, B. F., Burstein, S., Vasko, M. R., Prieto, A. L., O'Dell, D. K., and Walker, J. M. (2008) *N*-palmitoyl glycine, a novel endogenous lipid that acts as a modulator of calcium influx and nitric oxide production in sensory neurons. *Mol. Pharmacol.* **74,** 213–224
37. Saghatelian, A., McKinney, M. K., Bandell, M., Patapoutian, A., and Cravatt, B. F. (2006) A FAAH-regulated class of *N*-acyl taurines that activates TRP ion channels. *Biochemistry* **45,** 9007–9015
38. Oprescu, A. I., Bikopoulos, G., Naassan, A., Allister, E. M., Tang, C., Park, E., Uchino, H., Lewis, G. F., Fantus, I. G., Rozakis-Adcock, M., Wheeler, M. B., and Giacca, A. (2007) Free fatty acid-induced reduction in glucose-stimulated insulin secretion: evidence for a role of oxidative stress *in vitro* and *in vivo*. *Diabetes* **56,** 2927–2937
39. Rubí, B., Antinozzi, P. A., Herrero, L., Ishihara, H., Asins, G., Serra, D., Wollheim, C. B., Maechler, P., and Hegardt, F. G. (2002) Adenovirus-mediated overexpression of liver carnitine palmitoyltransferase I in INS1E cells: effects on cell metabolism and insulin secretion. *Biochem. J.* **364,** 219–226
40. Herrero, L., Rubí, B., Sebastián, D., Serra, D., Asins, G., Maechler, P., Prentki, M., and Hegardt, F. G. (2005) Alteration of the malonyl-CoA/carnitine palmitoyltransferase I interaction in the β-cell impairs glucose-induced insulin secretion. *Diabetes* **54,** 462–471
41. Yabuki, C., Komatsu, H., Tsujihata, Y., Maeda, R., Ito, R., Matsuda-Nagasumi, K., Sakuma, K., Miyawaki, K., Kikuchi, N., Takeuchi, K., Habata, Y., and Mori, M. (2013) A novel antidiabetic drug, fasiglifam/TAK-875, acts as an ago-allosteric modulator of FFAR1. *PLoS ONE* **8,** e76280
42. Alquier, T., Peyot, M. L., Latour, M. G., Kebede, M., Sorensen, C. M., Gesta, S., Ronald Kahn, C., Smith, R. D., Jetton, T. L., Metz, T. O., Prentki, M., and Poitout, V. (2009) Deletion of GPR40 impairs glucose-induced insulin secretion *in vivo* in mice without affecting intracellular fuel metabolism in islets. *Diabetes* **58,** 2607–2615